Control of trailing-edge separation by tangential blowing inside the bubble

P. R. Viswanath and K. T. Madhavan
Experimental Aerodynamics Division
National Aerospace Laboratories
Bangalore, India

ABSTRACT

Experiments have been performed investigating the effectiveness of steady tangential blowing, with the blowing slot located downstream of separation (but inside the separation bubble) to control a trailing-edge separated flow at low speeds. Trailing-edge separation was induced on a two-dimensional aerofoil-like body and the shear layer closure occurred in the near-wake. Measurements made consisted of model surface pressures and mean velocity, turbulent shear stress and kinetic energy profiles in the separated zone using a two-component LDV system. It is explicitly demonstrated that the novel concept of tangential blowing inside the bubble can be an effective means of control for trailing-edge separated flows as well. Blowing mass and momentum requirements for the suppression of wall and wake flow reversals have been estimated.

NOMENCLATURE

b	blowing slot height
C_D	sectional drag coefficient
C_p	static pressure coefficient $(p - p_\infty)/q_\infty$
C_μ	blowing momentum coefficient (2D)
C_f	wall skin friction coefficient
m_{bl}	boundary-layer mass flow rate
m_j	jet mass flow rate
p	local surface pressure
p_∞	freestream static pressure
q_∞	freestream dynamic pressure
U	local velocity in the boundary layer
U_∞	freestream velocity
U_j	jet velocity
$\langle u'^2 \rangle$	mean square velocity fluctuation in x direction
$\langle v'^2 \rangle$	mean square velocity fluctuation in y direction
$\langle u'v' \rangle$	Reynolds shear stress
x	co-ordinate parallel to model axis
y	co-ordinate normal to model axis
z	co-ordinate in spanwise direction
δ	boundary-layer thickness
θ	boundary-layer momentum thickness

1.0 INTRODUCTION

Turbulent boundary layer separation occurs in a variety of flow situations, for example, on aerofoils/wings at high incidence, intakes at supersonic speeds and afterbodies at transonic speeds; separation leads to energy losses, instability and other unsteady effects which are undesirable in engineering applications. Control of separated flows has become an active area of research triggered by technological needs. The monograph by Chang[1] contains an excellent account of several passive and active methods of separation control in different speed regimes. Recent reviews on the subject include that of Gad-El-Hak and Bushnell[2], Wygnanski and Seifert[3] and Greenblatt and Wygnanski[4].

Steady tangential blowing and boundary-layer suction have been widely explored to control separated flows[1]. Tangential blowing, which involves addition of fluid at the wall through a narrow slot, is generally known to be a useful control means; the injected mass energises the boundary layer near the wall providing sufficient kinetic energy to negotiate adverse pressure gradients. Earlier studies[5,6] have shown that, among various factors that influence blowing effectiveness, the injection or blowing slot location is a critical parameter. In the classical boundary layer control approach, the boundary layer is energised upstream or ahead of the separation location (Fig. 1(a)); some of the difficulties in using this conventional approach at high speeds have been noted by Viswanath *et al*[5]. Following these early observations[6], Viswanath *et al*[7] demonstrated recently through detailed flow-field measurements in an axisymmetric separated flow that injection or blowing downstream

Paper No. 2887. Manuscript received 17 March 2004, accepted 11 June 2004.

https://doi.org/10.1017/S0001924000000233 Published online by Cambridge University Press

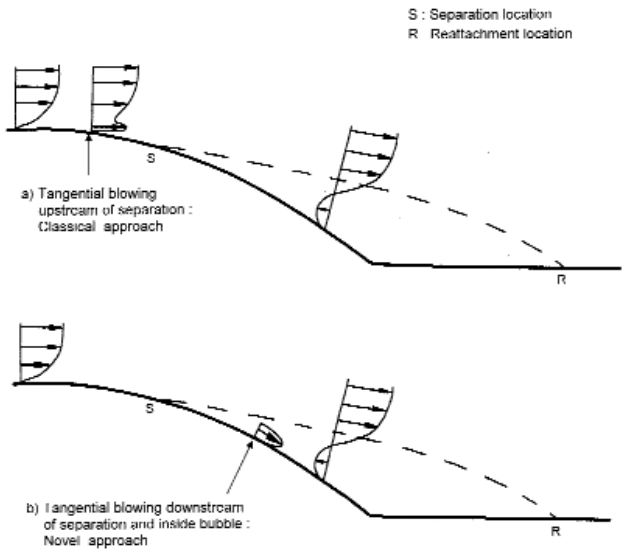


Figure 1. Schematic of tangential blowing concepts for separation control.

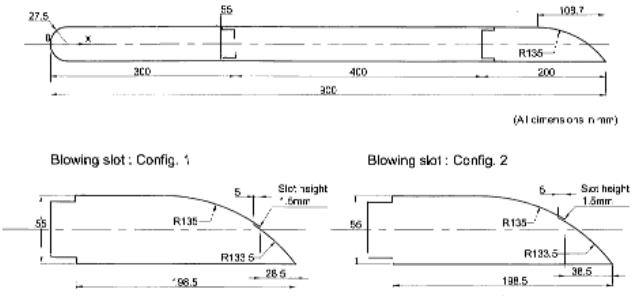


Figure 2. Geometric details of flat plate-contoured aft-section.

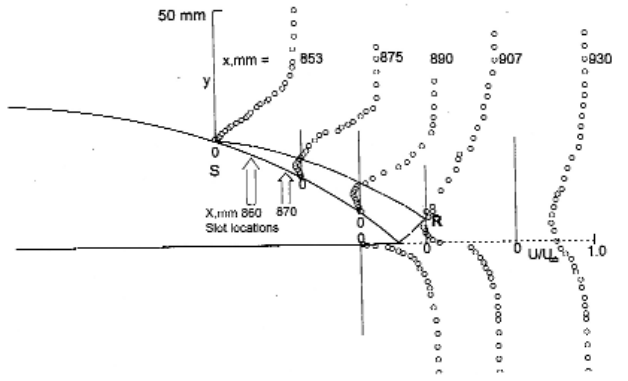


Figure 3. Mean velocity profiles in the separated zone without blowing (blowing slots shown).

of separation, but inside the bubble (Fig. 1(b)) can be an effective means of separation control. They[7] showed that wall flow reversal can be suppressed using injected mass of about 8% of the mass flow in the boundary layer at separation; complete wall and wake flow reversals were suppressed for an injected or jet mass flow ratio of about 13%. In the above experiment[7], the separated shear layer reattached on an axisymmetric sting, thus providing a solid wall boundary condition at reattachment.

In this paper, we have extended the applicability of this new concept of tangential blowing inside the bubble for separation control with shear layer or wake closure occurring in the near-wake of an aerofoil-like body; such a flow situation will be relevant to separation control on aerofoils and wings. Detailed flow-field measurements using a two-component LDV system have been made in the separated zone for two positions of blowing slot, thus optimising the blowing performance. Blowing mass and momentum requirements for the suppression of wall and wake flow reversals have been estimated. It is demonstrated that tangential blowing inside the bubble can be an effective means of separation control for trailing-edge separated flows as well.

2.0 EXPERIMENTS

2.1 Wind tunnel and flat plate model

The experimental study was conducted in the 0·55m × 0·55m low speed wind tunnel. The model configuration employed was a long 2D flat-plate (spanning the tunnel width) with a contoured aft-section (Fig. 2); the aft-section (with a length of 0·108m) has a circular arc on the upper surface with a radius of curvature of 0·135m, providing adequate adverse pressure gradients for the turbulent boundary-layer to separate well ahead of the trailing-edge. The turbulent boundary-layer on the flat plate ahead of the contoured section was relatively thick and well developed.

2.2 Contoured aft-section models with blowing slots

Two contoured aft-section models for tangential blowing experiments were designed (Fig. 2). Initial experiments revealed that boundary-layer separation occurred on the basic contoured aft-section model (without blowing slot) around x = 853mm and shear layer closure at x = 907mm (see Fig. 3). Two blowing slot configurations were chosen with the slot located within the bubble (Fig. 3) based on earlier work[5,7]

Config. 1 : slot located at x = 870mm with slot height (b) of 1·5mm
Config. 2 : slot located at x = 860mm with slot height (b) of 1·5mm

The geometric details of the two contoured aft-section models are included in Fig. 2 and the blowing slot also spanned the tunnel width. Considerable care was taken in the design of the slot to ensure tangential blowing. The flat plate model including the aft-section contoured sections were instrumented with a large number of static pressure taps (of 0·8mm i.d.) on the model centreline. Limited spanwise pressure taps on the top surface of the contoured section, over the mid 25% of the span, were provided as well.

2.3 Instrumentation

The model static pressure distributions were measured using two Furness Control micro-manometers. Flow-field measurements involving mean velocity, turbulent shear stress and kinetic energy profiles in the separated zone and near-wake were carried out using a three-beam, two-component DANTEC Laser Velocimeter; a schematic of LDV system and data processing is shown in Fig. 4. The LDV system was used in the forward scatter mode to achieve high signal to noise ratio. The focal length of the front lens was 600mm and the beam intersection angle was 4·66°. The ellipsoidal probe volume had a length of about 2mm and a diameter of 0·2mm. Fringe spacing in the blue and green components were 6·8 and 7·2μm respectively. A Bragg cell with an optical frequency shift of

https://doi.org/10.1017/S0001924000000233 Published online by Cambridge University Press

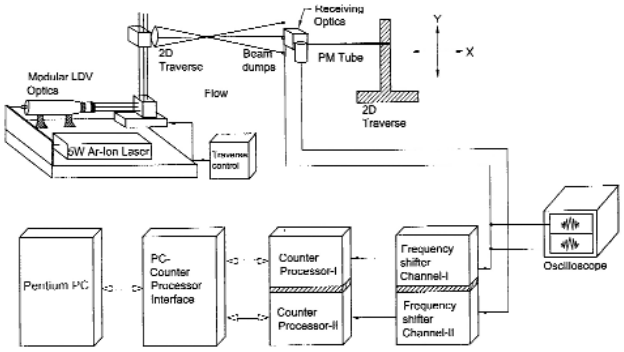
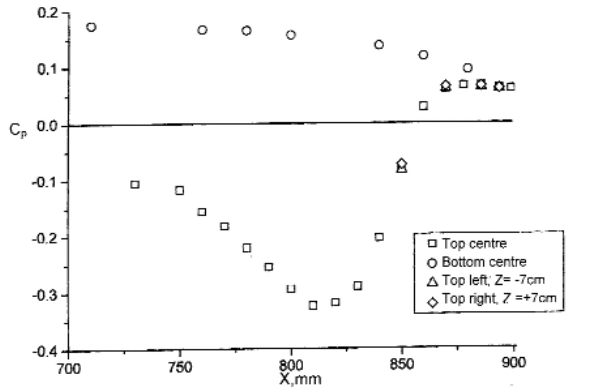
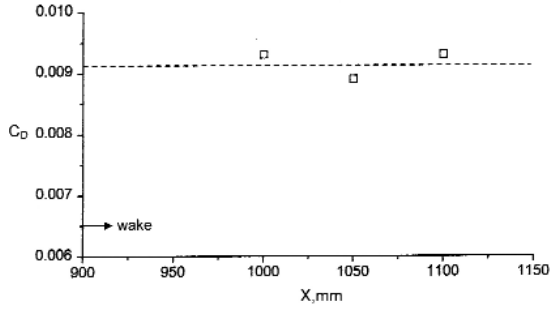


Figure 4. Schematic of LDV system and data processing.



a) Comparison of streamwise and spanwise surface pressure distributions : Basic model



b) Variation of drag coefficient in the wake : Basic model

Figure 5. Results of mean flow two dimensionally.

40MHz was used for measuring the reversed flow; in addition, an electronic frequency shift was also used for accurate measurement of low velocities. Data from the counter-type signal processor was transferred to the PC/AT system using DMA-based high-speed digital I/O cards.

The mean velocity, turbulent shear stress and two-component turbulent kinetic energy profile measurements were made on the basic aft-section model (without blowing slot) and on Config. 2 (with blowing slot located at x = 860mm) with laser beam optics in the ±45° configuration; on Config. 1 (with blowing slot located at x = 870mm), only mean velocity measurements were made. Seeding was accomplished successfully using the well known Eurolite smoke fluid which provided good particle concentration even within the recirculating zones of the flow. No direct estimate of the particle sizes was made; however, we expect that the particle size is in the range of 5 to 20 microns. The data rates were typically in the range 400 to 600 samples/s. Data validation rates were in the range of 500 to 800 for a batch of 1,000 samples, which is generally indicative of good SNR conditions. Although an ensemble size of about 1,000 samples was adequate for the accurate determination of mean velocities in forward and reversed flow zones, ensemble size of about 3,000 samples was utilised in the present study in order to significantly enhance the quality and accuracy of turbulence parameters like the shear stress and kinetic energy.

2.4 Test conditions

The experiments were performed at a freestream velocity (U_∞) of 25ms^{-1}, providing a model chord Reynolds number of 1×10^6. Two blowing jet velocity (U_j) of $0{\cdot}75U_\infty$ and $1{\cdot}0\ U_\infty$ were used to assess blowing effectiveness.

2.5 Two-dimensionality

Mean flow two-dimensionality was assessed by the following measurements:

(*i*) the spanwise surface pressures in the separated zone showed good agreement with centreline values (Fig. 5(a));
(*ii*) the separation[8] line, as visualised using a surface flow technique (titanium-di-oxide in oil), showed[8] very good spanwise uniformity over mid 60% model span and
(*iii*) drag values of the model (without blowing) determined from mean velocity survey at different streamwise stations in the wake were about the same (within ±2% (Fig. 5(b))).

These observations suggest excellent mean flow two-dimensionality in the experiments.

2.6 Measurement uncertainties

For the LDV data, sources of error include optical, statistical and positional. The uncertainty in the measurement of beam half-angle is estimated to be ±0·01° which translates to an uncertainty in velocity of ±0·05m/s; however, the resolution of the burst counter results in a relatively higher uncertainly of ±0·1ms^{-1}. For the sample size used for each data point (discussed above) we expect the statistical errors to be small (<1%). No correction for the measured data for possible velocity bias was made since such corrections did not seem warranted based on comparisons of measurements in certain standard flows as well as redundancy measurements[9]; such an observation has also been made by Adams and Eaton[10] in a low speed separated flow. Furthermore, reliable corrections schemes are not established for velocity bias. Likely errors in the measured mean velocity, turbulent shear stress and two-component kinetic energy data are given below; these estimates are based on repeatability tests and comparison with redundancy measurements, wherever possible.

Pressure coefficient, C_p	< ±0·3%
Mean velocity, U	< ± 2% or 0·1ms^{-1} whichever is higher
Turbulent shear stress	< ±6%
Turbulent kinetic energy	< ±8%
x	< ± 0·5mm
y	< ± 0·3mm

https://doi.org/10.1017/S0001924000000233 Published online by Cambridge University Press

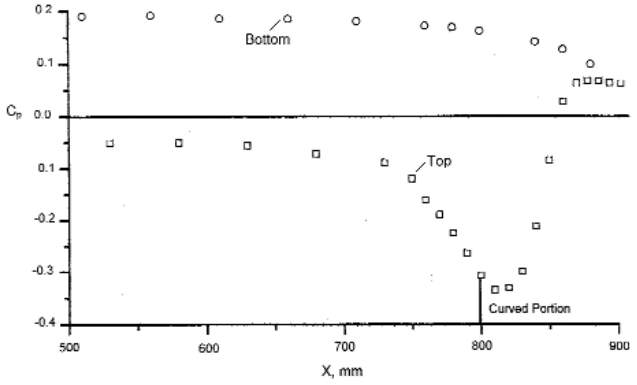


Figure 6. Model static pressure distribution without blowing.

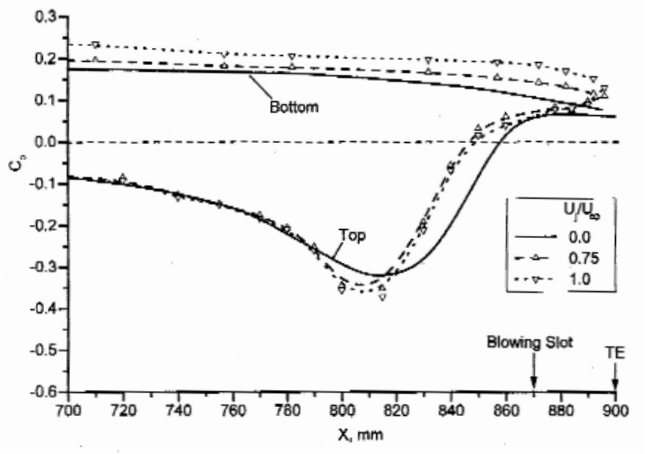


Figure 7. Effect of blowing on model static pressure distribution: Config. 1.

3.0 RESULTS AND DISCUSSION

3.1 Boundary-layer properties on the flat plate

The measured mean velocity profile in the flat plate region on the model upper surface at x = 590mm was determined from pitot measurements. The velocity profile showed[8] the standard logarithmic law with a wake defect suggesting a fairly well developed turbulent boundary-layer ahead of the contoured aft-section. The boundary-layer parameters were: total thickness, δ = 20mm, displacement thickness, δ^* = 2·03mm, momentum thickness, θ = 1·58mm, shape factor = 1·28 and wall skin friction coefficient, C_f = 0·0035.

3.2 Results on the basic model without blowing

3.2.1 Surface pressure distributions

The measured static pressure distributions on the model, over a distance of 400mm upstream of the trailing edge, are presented in Fig. 6. As may be observed, the model generates some lift since it is positively cambered. The pressure distribution is uniform on the top and bottom flat plate sections, but at different levels. On the top surface, the pressure decreases gradually towards the beginning of the contoured aft-section due to the sudden change in surface curvature and is followed by a strong adverse pressure gradient along the contoured surface leading to boundary-layer separation, as observed by the pressure plateau ahead of the model trailing-edge. The surface flow visualisation studies indicated[8] a mean separation line at x = 853 ±2mm.

3.2.2 Mean velocity profiles

The mean velocity profiles measured at selected streamwise stations (Fig. 3) shows that boundary-layer separation (S) occurred around x = 853mm and shear layer closure (R) at x = 907mm. The relatively rapid wake closure occurs because of the interaction of the separated shear layer with the energetic lower surface turbulent boundary-layer. The profile at x = 890mm shows clearly reversed flow zone with a height of about 10mm from the model surface. The velocity profile at x = 907mm shows strong normal velocity gradients and quick recovery follows in the near-wake at x = 930mm downstream of wake closure.

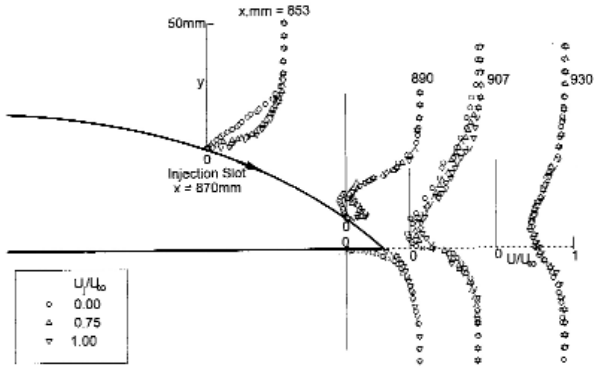


Figure 8. Effect of blowing on mean velocity profiles: Config. 1.

3.3 Results with blowing: Config. 1

3.3.1 Static pressure distributions

Fig. 7 presents the measured model static pressure distributions at the two values of $U_j = 0{\cdot}75$ and $1{\cdot}0U_\infty$; also shown for comparison is the pressure distribution on the basic configuration without blowing. The pressure distributions, while being qualitatively similar to the no blowing case, reveal the following features due to blowing:

(*i*) surface pressures on the top surface of the model are unaffected ahead of x = 770mm;
(*ii*) the pressure rise on the contoured section (following C_{pmin}) is relatively more steeper initially at both blowing velocities;
(*iii*) the pressure plateau is eliminated and pressure rise occurs gradually all the way upto the trailing-edge, suggesting elimination of wall flow reversal; and
(*iv*) model trailing-edge pressures are higher with blowing. As a result of attached flow up to the trailing edge, the overall circulation around the model is improved and relatively higher surface pressure values on the model lower surface can be observed as well. Essentially, tangential blowing has not only suppressed wall flow reversal resulting in pressure recovery upto the trailing edge, but also has improved the overall circulation around the model.

https://doi.org/10.1017/S0001924000000233 Published online by Cambridge University Press

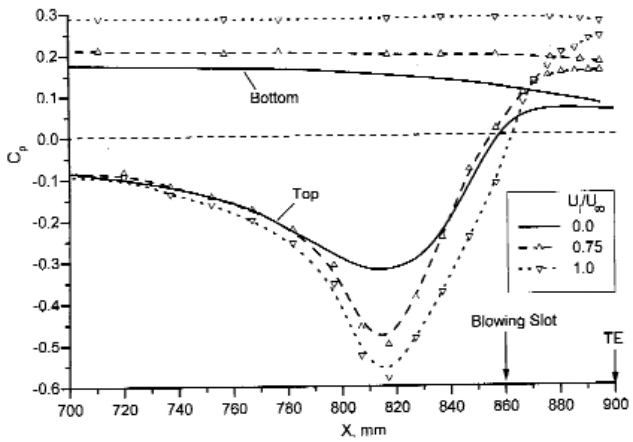


Figure 9. Effect of blowing on model static pressure distribution: Config. 2.

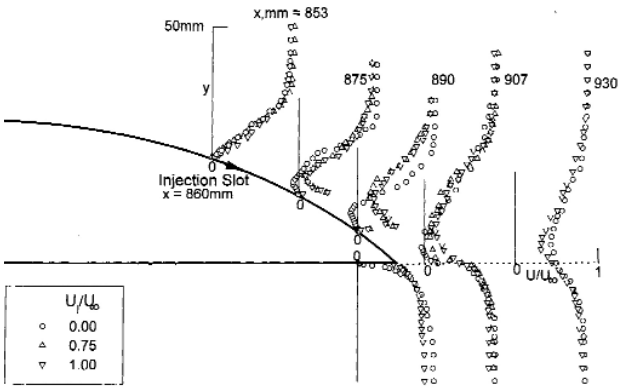


Figure 10. Effect of blowing on mean velocity profiles: Config. 2.

3.3.2 Mean velocity profiles

The mean velocity profiles with blowing are presented in Fig. 8; the results of mean velocity without blowing are included in order to bring out the effect of blowing. The velocity profiles at separation (x = 853mm) are much fuller near the wall and absence of reversed flow at x = 890mm is clearly seen at both values of U_j. Increased velocities at wake closure location (x = 907mm) is to be expected since boundary-layer separation is suppressed by blowing. The velocity profiles with $U_j = U_\infty$ in general show slightly higher values, as may be expected compared to $U_j = 0{\cdot}75U_\infty$. The velocity profile at x = 890mm on the lower surface is appreciably fuller near the wall due to blowing, possibly as a result of the strong interaction between the upper and lower surface boundary-layers. The results shown in Fig. 8 do show absence of both wall and wake flow reversal particularly at $U_j = U_\infty$.

3.4 Results with blowing: Config. 2

3.4.1 Static pressure distributions

The pressure distributions at both blowing velocities of 0·75 and $1{\cdot}0U_\infty$. (Fig. 9), while being qualitatively similar to Config. 1 (Fig. 7), show larger effects. The surface pressure values around C_{pmin} are appreciably lower, and the pressure recovery at the trailing edge much higher compared to Config. 1. As a result, the circulation around the model is larger (relative to Config. 1) at both values of U_j, with higher lift enhancement for $U_j = U_\infty$. The adverse pressure gradients on the contoured section are relatively higher comparable to Config. 1 (with blowing), and once again, the absence of pressure plateau (at both values of U_j) suggests that the wall flow reversal is eliminated by blowing.

3.4.2 Mean velocity profiles

For blowing Config. 2, (with slot location closer to separation), the velocity profile at separation (x = 853mm) show relatively smaller improvements due to blowing (Fig. 10) unlike in Config. 1. However, the beneficial effects of blowing are more clearly observed at x = 875 and 890mm; both wall and wake flow reversals are eliminated at both values of U_j and the velocity levels near the wall are much larger than with those seen with Config. 1 (Fig. 8). The wake closure is naturally eliminated with blowing. The outer layers at x = 875 and 890mm show visible retardation of the boundary-layer flow since the adverse pressure gradient on the contoured section is much steeper and extended (Fig. 9) compared to the no blowing case. Since the pressure recovery is higher at the trailing edge, the boundary-layer edge velocities at x = 875 and 890mm are slightly lower compared to the no blowing case. As with Config. 1, the velocity profile on the lower surface at x = 890mm is appreciably fuller due to blowing, as a result of the interaction with the upper surface boundary-layer which is attached.

It is useful and appropriate to mention the aerodynamic benefits resulting from blowing for this case which appears optimal. With trailing-edge separation completely suppressed, the lift generated on the model may be inferred to be appreciably higher (Fig. 9); in particular, the lift increase on the contoured aft-section was about 70% at $U_j = U_\infty$ (compared to the no blowing case). With regard to the total drag of the model (estimated from wake velocity profiles at x = 930mm, Fig. 10), it is slightly higher (about 3% of $U_j = U_\infty$) which is to be expected since the boundary-layer on the contoured section has undergone a relatively higher adverse pressure gradient all the way up to the trailing-edge. In essence, the lift to drag ratio of the model is considerably enhanced by blowing with trailing-edge separation suppressed.

3.4.3 Turbulent shear stress and kinetic energy profiles

Turbulent shear stress and two-component kinetic energy profiles were measured on the blowing Config. 2, which was found to be more effective in suppressing trailing-edge separation; these measurements were made for the case of $U_j = U_\infty$. The results of normalised turbulent shear stress and turbulent kinetic energy profiles are shown (except at x = 930mm and x = 890mm (lower surface)) in Figs 11 and 12, respectively; results for the no blowing case are included for comparison. The complex qualitative nature of the shear stress profiles can be explained from the corresponding mean velocity profiles with blowing (Fig. 10). At x = 853mm, the shear stress profiles show features typical for a retarded attached boundary-layer. The shear stress profiles at x = 875 and 890mm show two peaks corresponding to the positive and negative maximum (normal) velocity gradients of the mean flow; these profiles result from a wake-like behaviour of the velocity field with a velocity minimum (Fig. 10). A third peak in (positive) shear stress very close to the wall in the jet-boundary-layer has not been captured in the measurements since it occurs very close to the wall (y < 0·5mm). Following merging of the top and bottom shear layers at the trailing-edge, the profiles show lower normal shear stress gradients and lower values for the two peaks, as expected (x = 907mm). The shear stress peaks further diminish at x = 930mm as a result of the wake growth and the profile is appreciably asymmetric.

https://doi.org/10.1017/S0001924000000233 Published online by Cambridge University Press

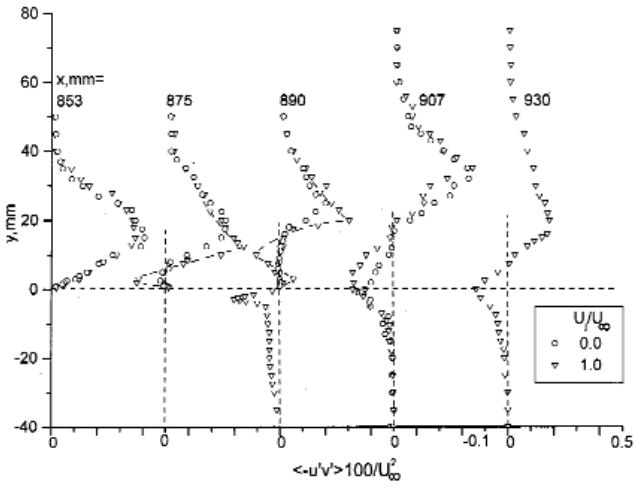


Figure 11. Effect of blowing on turbulent shear stress profiles: Config. 2.

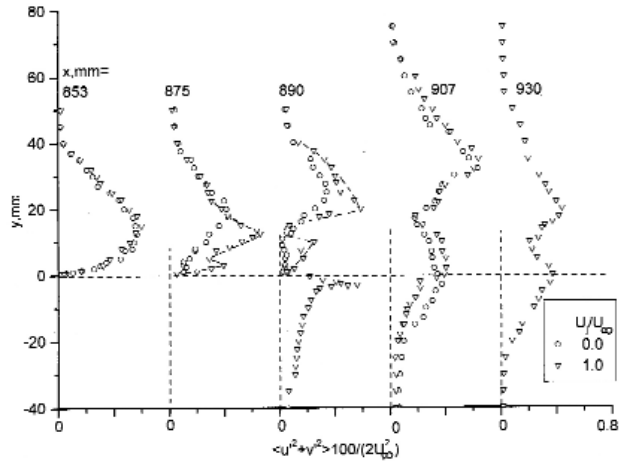


Figure 12. Effect of blowing on turbulent kinetic energy profiles: Config. 2.

The kinetic energy profiles (Fig. 12) show certain features similar to the shear stress profiles which are to be expected. The changes in kinetic energy profile at x = 853mm are small consistent with the small changes in the velocity and turbulent shear stress profiles. At x = 875 and 890mm, two peaks are seen corresponding to the wall jet-boundary-layer and outer layer and the levels are significantly higher due to increased mixing in the presence of blowing. As with shear stress profiles, following merging, the normal gradients of kinetic energy are lower and the peak values are reduced as the wake develops downstream.

The above features of turbulent shear stress and kinetic energy profiles with blowing show broad similarities with those observed in an axisymmetric separated flow with blowing (Ref. 7).

3.5 Blowing requirements

In the context of separation control, elimination of wall flow reversal may be adequate in certain applications, while elimination of both wall and wake flow reversals may be needed in other cases (e.g. aircraft intakes). Here, we define blowing momentum coefficient, C_μ, as

Table 1
Estimates of blowing mass and momentum: blowing inside bubble

Model geometry	m_j/m_{bl}	C_μ	Remarks
2D Comp. Corner (Ref. 5) M_∞ = 2·40	18%	-	Shear layer reattachment on solid surface; inadequate information to estimate C_μ
Axisym. (Ref. 7) $M_\infty \sim 0$	13%	0·90	Shear layer reattachment on solid surface; C_μ estimated in a 2D sense (Equation (1))
2D (Present) $M_\infty \sim 0$	5%	0·33	Shear layer closure in the near-wake

$$C_\mu = m_j U_j / \rho_0 U_0^2 \theta_0 \qquad ...(1)$$

where m_j is the jet mass flow rate per unit span, U_j is the jet velocity, ρ_0 and U_0 are the local freestream density, velocity just ahead of separation point and θ_0 is the local boundary-layer momentum thickness. In the above definition of C_μ, we have utilised a viscous scale θ_0 for normalisation, being more appropriate for reflecting local dynamics of the mean flow (as opposed to using an inviscid length scale associated with the model configuration; see Chapter 5.3, Ref. 1).

Estimates of blowing mass and momentum requirements for the suppression of both wall and wake flow reversals are given in Table 1. Estimates for the supersonic case (Ref. 5) and axisymmetric separation case (Ref. 7), both involving tangential blowing inside the bubble are included in the Table for a broad comparison.

The results shown above suggest a decreasing requirement of normalised jet mass flow with decreasing freestream Mach number. The value of C_μ for the axisymmetric case (Ref. 7) is higher both because of larger blowing velocity requirements needed to suppress both wall and wake flow reversals and higher slot width (compared to the present experiments).

While it would be useful to compare the effectiveness of blowing studied here with other forms of blowing reported in literature, it is generally a difficult task since the effectiveness would depend on a host of parameters including flow configuration, scale of separation, pressure gradient history and Reynolds number. Test results on trailing-edge separation (comparable to the present experiments) with other forms of blowing are not available and hence such a comparison is not attempted here. The relatively low values of C_μ needed to suppress separation (see Table 1) suggest strongly that the requirements are comparable to those available in published literature (e.g. Ref. 1). It is also to be noted that the values C_μ (Table 1) will be significantly lower (by a factor of 500-1,000) if the model chord (inviscid length scale) is utilised for non-dimensionalising C_μ instead of θ_o.

4.0 CONCLUSIONS

The new experimental results have explicitly demonstrated that the novel approach of tangential blowing, with the slot located downstream of the separation point but inside the bubble, can be an effective means of separation control with shear layer closure occurring in the near-wake as well. The effectiveness of blowing inside the bubble in suppressing both wall and wake flow reversals seems remarkable even with a narrow slot (about 5% of local boundary-layer thickness); furthermore, blowing results in significant enhancement in the turbulent kinetic energy levels near the wall which could be a beneficial feature in applications.

The results show that the effectiveness of blowing is gradual with increasing jet velocity. The blowing Configuration 2, located relatively closer to the separation point, appears to be optimal especially

https://doi.org/10.1017/S0001924000000233 Published online by Cambridge University Press

concerning total suppression of the separated flow and higher lift generation on the model. Since the boundary-layer is attached at the trailing edge with blowing (for both slot locations), Kutta condition is satisfied and therefore results in larger beneficial changes, including improved circulation and lift on the model.

With the novel approach of blowing inside the bubble, it is the flow in the bubble (or dead air zone) which is energised leading to the eventual removal of shear layer closure, as opposed to energisation of the boundary-layer upstream of separation point, which is adopted in classical boundary-layer control. Manipulation of shear layer reattachment or closure is the 'Key Principle of Separation Control'. The flow mechanisms that may be responsible for the effectiveness of this blowing concept include:

(a) elimination of wall flow reversal due to the interaction of the injected jet (having higher total pressure or longitudinal momentum) with the reversed flow boundary-layer leading to surface pressure recovery;
(b) injection of mass into the bubble causes a strong mass imbalance affecting the shear layer entrainment characteristics ; and
(c) jet entrainment of the reversed flow in the bubble, a strong factor promoting increased mixing near the wall.

The above novel concept may have considerable potential as a means of controlling separated flows in other situations. The flow-field data of mean velocity, turbulent shear stress and kinetic energy profiles in the separated zone generated in this study could be very valuable in the development of improved turbulence modeling and validation of CFD codes.

ACKNOWLEDGEMENTS

This work was carried out from a grant received from the Aeronautical Research and Development Board, Government of India.

REFERENCES

1. CHANG, P.K. *Control of Flow Separation*, 1976, Hemisphere Publishing Corporation.
2. GAD-EL-HAK, M. and BUSHNELL, D.M. Separation control: review, *J Fluids Eng*, 1991, **113**, pp 5-30.
3. WYGNANSKI, I. and SEIFERT, A. Separation control by periodic addition of momentum, AIAA Paper 94-2608, 1994.
4. GREENBLATT, D. and WYGNANSKI, I.J. The control of flow separation by periodic excitation, *Prog Aerospace Sci*, 2000, **36**, pp 487-545.
5. VISWANATH, P.R., SANKARAN, L., SAGDEO, P.M., NARASIMHA, R. and PRABHU, A. Injection slot location for boundary-layer control in shock-induced separation, *J Aircr*, 1983, **20**, pp 726-732.
6. PEAKE, D.J. The use of air injection to prevent separation of turbulent boundary-layer in supersonic flow, ARC CP 890, 1966.
7. VISWANATH, P.R., RAMESH, G. and MADHAVAN, KT. Separation control by tangential blowing inside the bubble, *Experiments in Fluids*, 2000, **29**, pp 96-102.
8. VISWANATH, P.R. and MADHAVAN, K.T. Control of airfoil-type separated flow by tangential blowing, National Aerospace Laboratories Report PD EA 0109, 2001.
9. RAMESH, G., MADHAVAN, K.T. and VISWANATH, P.R. LDV measurements in an axisymmetric separated flow, Part I: Without flow control, National Aerospace Laboratories Report PD EA 9505, 1995
10. ADAMS, E.W. and EATON, J.K. An LDV study of the backward facing step flow including the effects of velocity bias, *J Fluids Eng*, 1988, **110**, pp 275-282.

https://doi.org/10.1017/S0001924000000233 Published online by Cambridge University Press